Supplementary Information

Rational design of NiFe LDH@Ni_3N nano/microsheet arrays as bifunctional electrocatalyst for overall water splitting

Boran Wang,[a] Shihui Jiao,[a] Zisheng Wang,[a] Mengjie Lu,[b] Duo Chen,[b] Yutang Kang,[a]

Guangsheng Pang*[a] and Shouhua Feng[a]

[a] *The State Key Laboratory of Inorganic Synthesis and Preparative Chemistry, College of Chemistry, Jilin University, Changchun 130012, P. R. China.*

[b] *Sino-Russian International Joint Laboratory for Clean Energy and Energy Conversion Technology, College of Physics, Jilin University, Changchun 130012, P. R. China.*

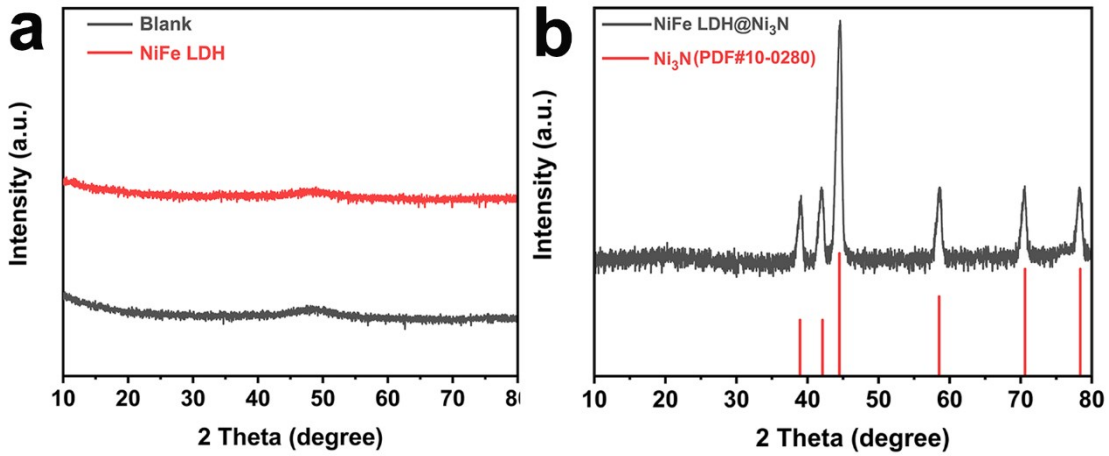

Figure S1. XRD patterns of (a) the NiFe LDH powder and blank substrate and (b) the NiFe LDH@Ni_3N powder.

To eliminate the effect of Ni foam, we peeled the NiFe LDH and NiFe LDH@Ni_3N from the NiFe LDH/NF and NiFe LDH@Ni_3N/NF, respectively. There are no observable peaks in the XRD pattern of the NiFe LDH powder. The XRD pattern of the NiFe LDH@Ni_3N powder peeled from Ni foam verifies the Ni_3N phase. No observable diffraction peaks of NiFe LDH can be found from the corresponding XRD pattern.

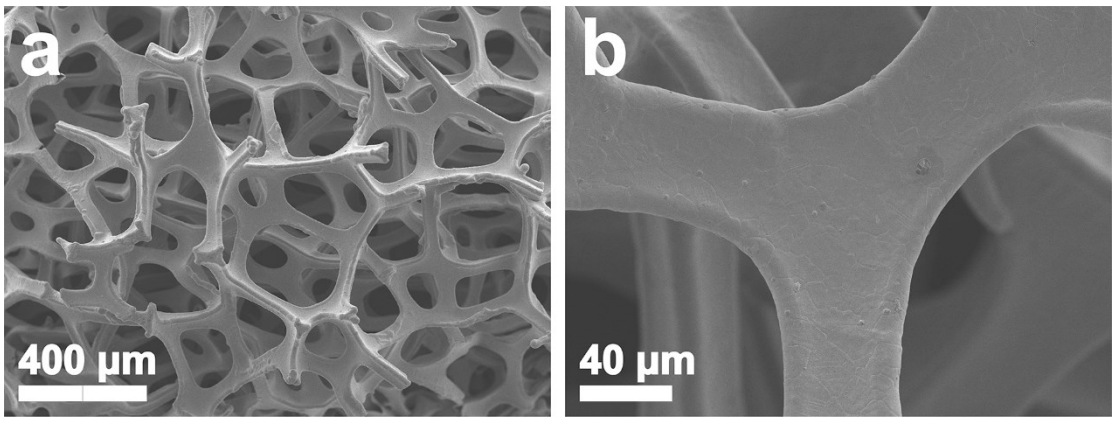

Figure S2. SEM images of the commercial Ni foam.

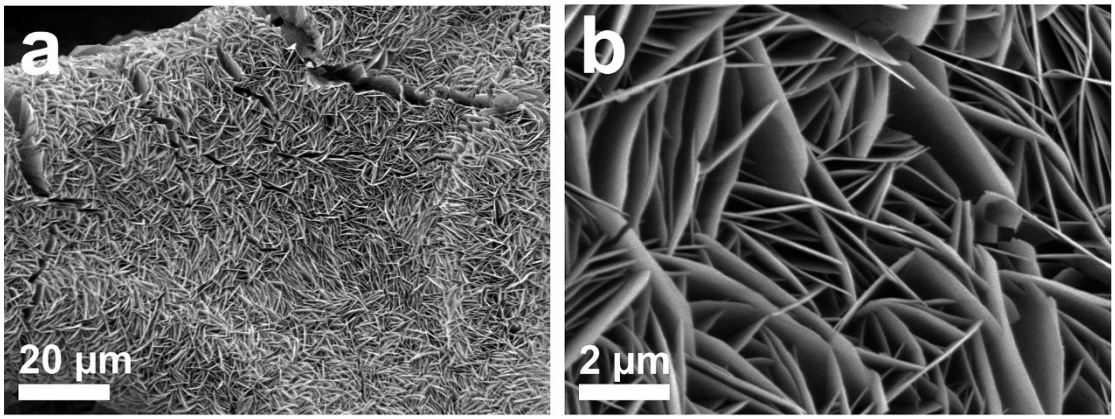

Figure S3. SEM images of the $Ni(OH)_2$/NF.

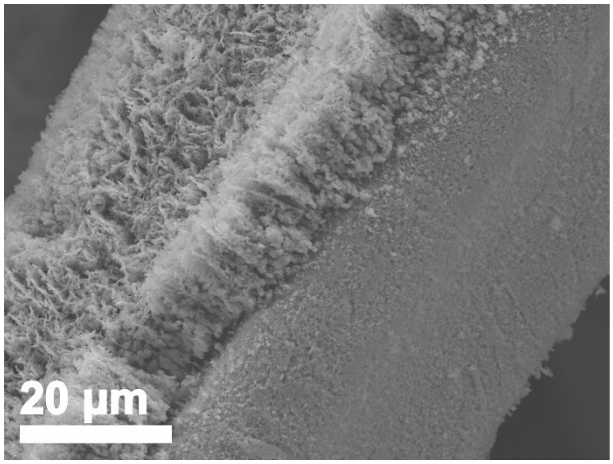

Figure S4. Cross-section SEM image of the NiFe LDH@Ni_3N/NF.

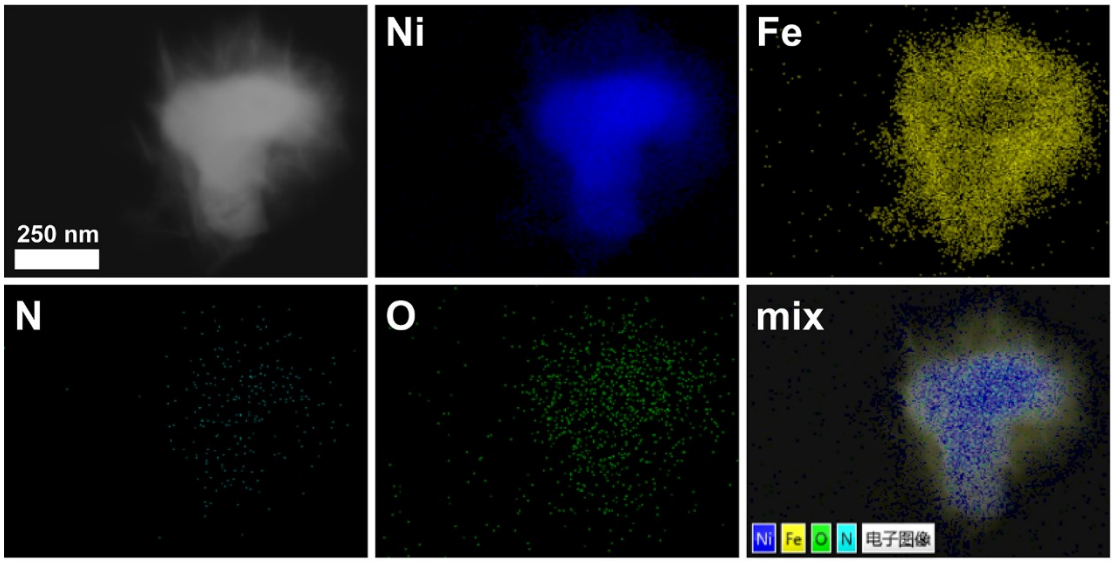

Figure S5. The scanning transmission electron microscopy image and the corresponding elemental mappings of Ni, Fe, N and O in the NiFe LDH@Ni_3N.

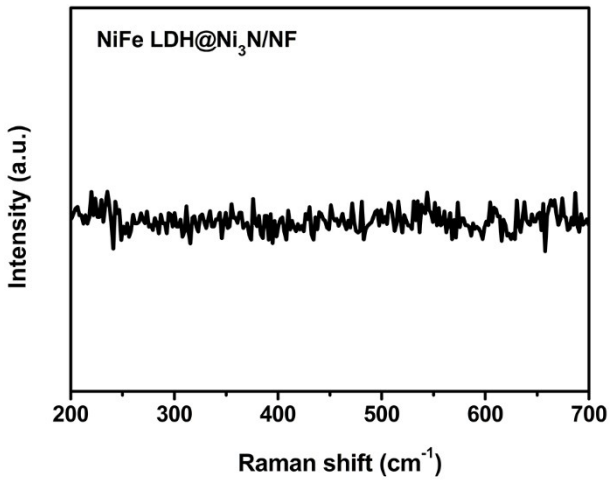

Figure S6. Raman spectrum of the NiFe LDH@Ni_3N/NF.

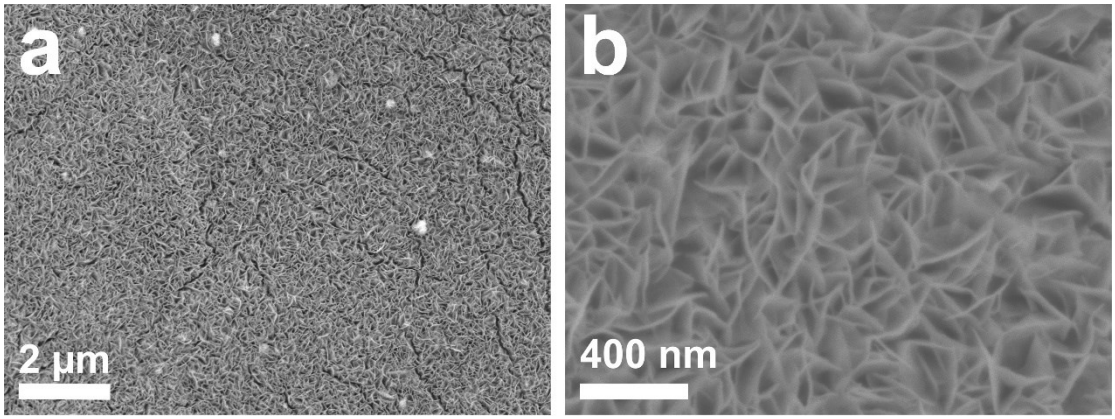

Figure S7. SEM images of the NiFe LDH/NF.

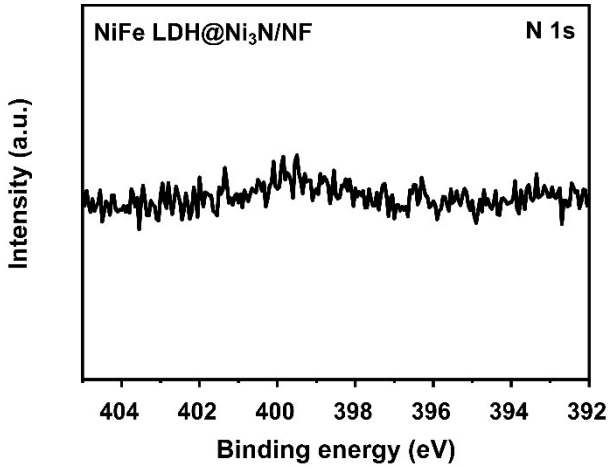

Figure S8. High-resolution XPS spectrum of N 1s for the NiFe LDH@Ni_3N/NF.

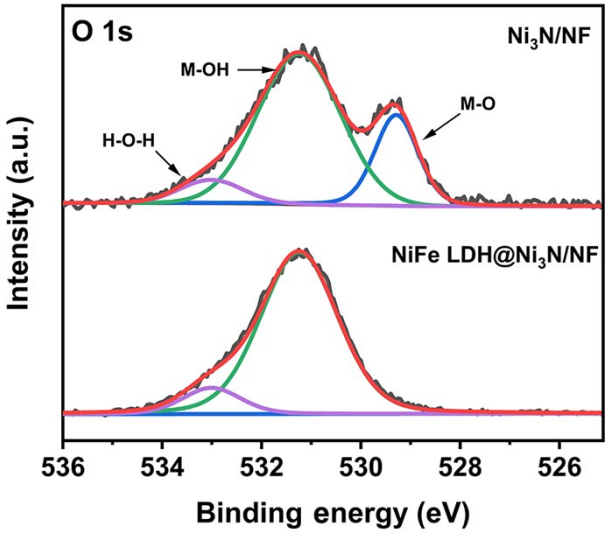

Figure S9. High-resolution XPS spectra of O 1s for the Ni_3N/NF and NiFe LDH@Ni_3N/NF.

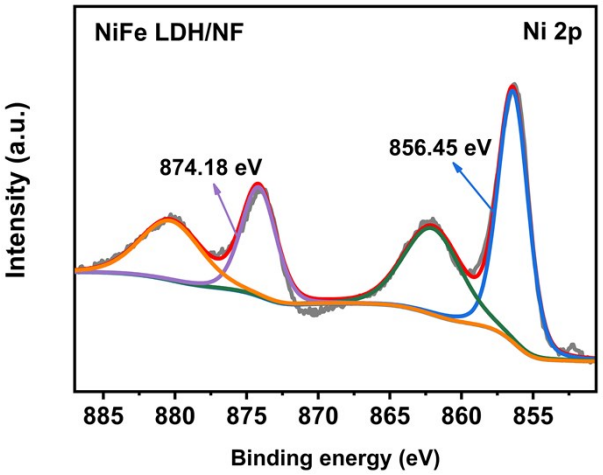

Figure S10. High-resolution XPS spectrum of Ni 2p for the NiFe LDH/NF.

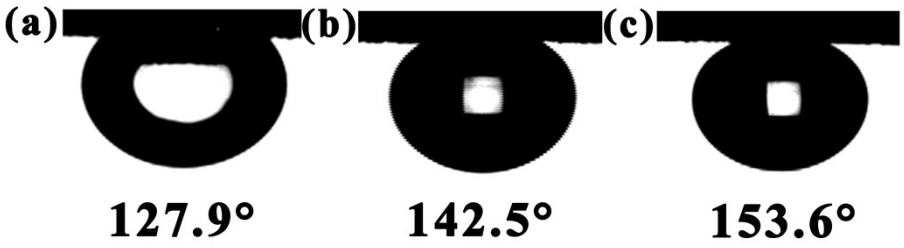

Figure S11. Air bubble contact angles under electrolyte at the (a) blank NF; (b) Ni_3N/NF and (c) NiFe LDH@Ni_3N/NF.

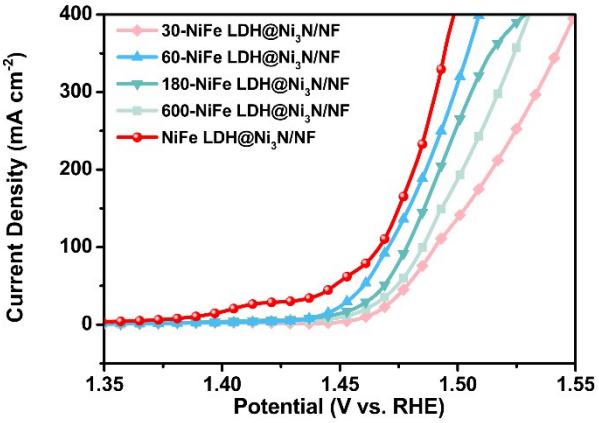

Figure S12. OER polarization curves of the 30-NiFe LDH@Ni_3N/NF, 60-NiFe LDH@Ni_3N/NF, 180-NiFe LDH@Ni_3N/NF, 600-NiFe LDH@Ni_3N/NF, and NiFe LDH@Ni_3N/NF electrode.

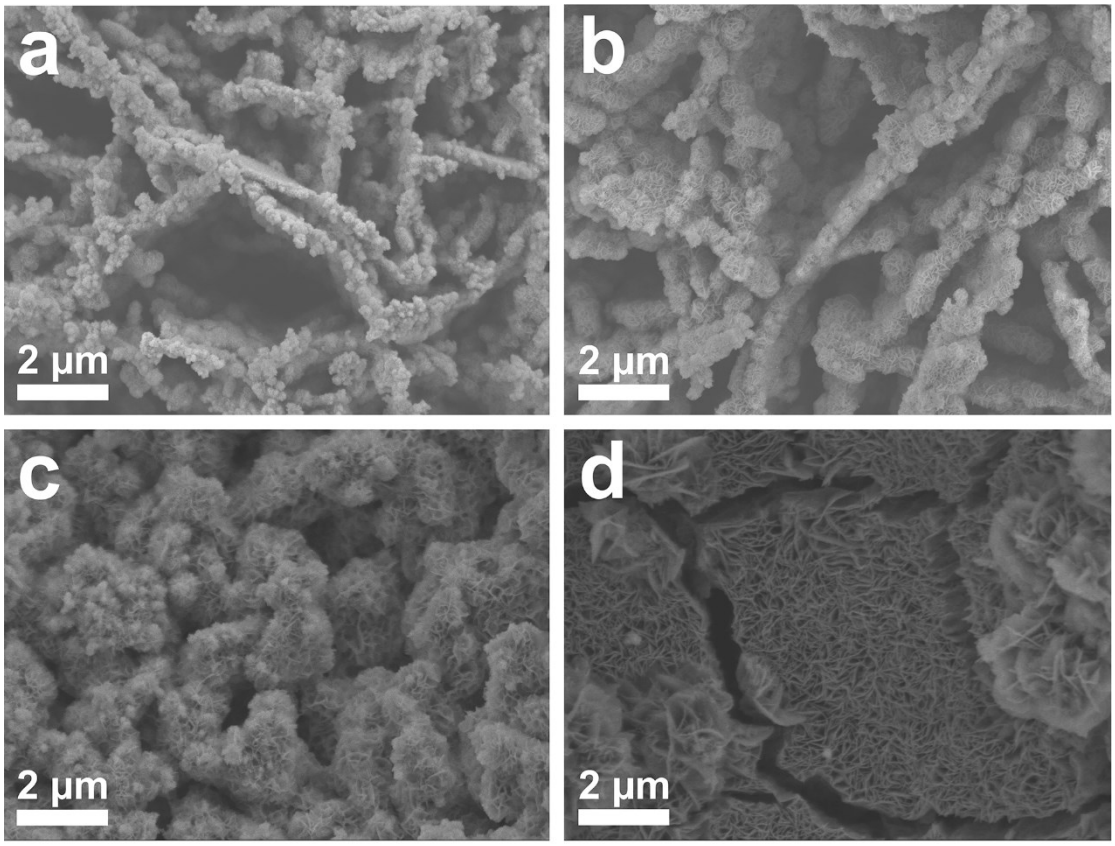

Figure S13. SEM images of (a) 30-NiFe LDH@Ni_3N/NF; (b) 60-NiFe LDH@Ni_3N/NF; (c) 180-NiFe LDH@Ni_3N/NF and (d) 600-NiFe LDH@Ni_3N/NF.

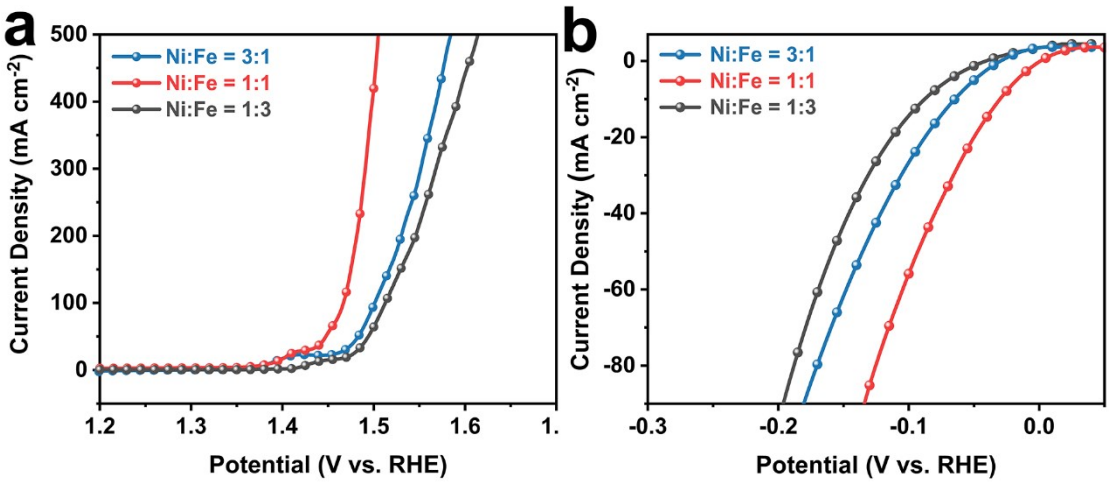

Figure S14. (a) OER and (b) HER polarization curves of the NiFe LDH@Ni_3N/NF catalysts synthesized with different initial Ni/Fe ratio.

To optimize the composition of the electrodeposited NiFe LDH nanosheets, we have used electrolyte with different Ni/Fe precursor ($Fe(NO_3)_3 \cdot 9H_2O$ and $Ni(NO_3)_2 \cdot 6H_2O$) ratio (e.g., 7.5 mM of Fe^{3+} and 22.5 mM of Ni^{2+}; 22.5 mM of Fe^{3+} and 7.5 mM of Ni^{2+}; 15 mM of Fe^{3+} and 15 mM of Ni^{2+}).

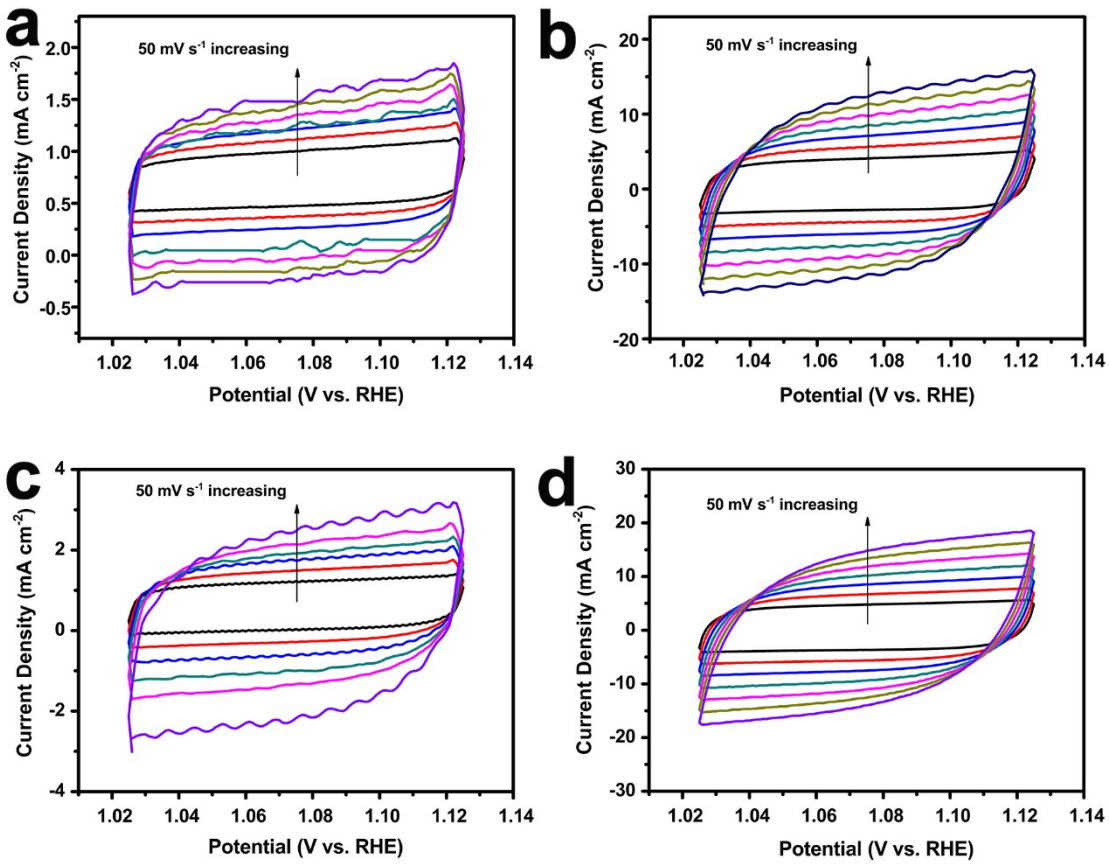

Figure S15. CV curves of the (a) blank NF; (b) Ni_3N/NF; (c) NiFe LDH/NF and (d) NiFe LDH@Ni_3N/NF measured at different scan rates.

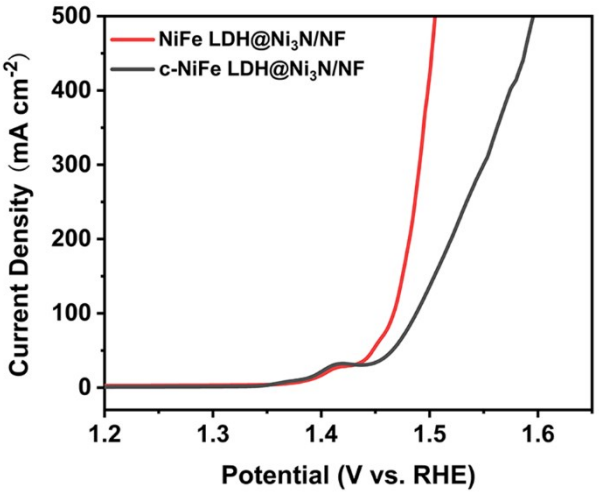

Figure S16. OER polarization curves of the NiFe LDH@Ni_3N/NF and the annealing sample.

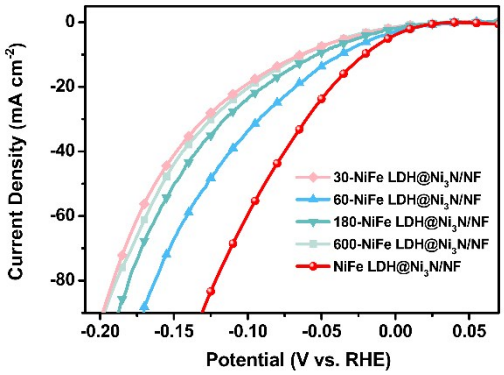

Figure S17. HER polarization curves of the 30-NiFe LDH@Ni_3N/NF, 60-NiFe LDH@Ni_3N/NF, 180-NiFe LDH@Ni_3N/NF, 600-NiFe LDH@Ni_3N/NF, and NiFe LDH@Ni_3N/NF electrode.

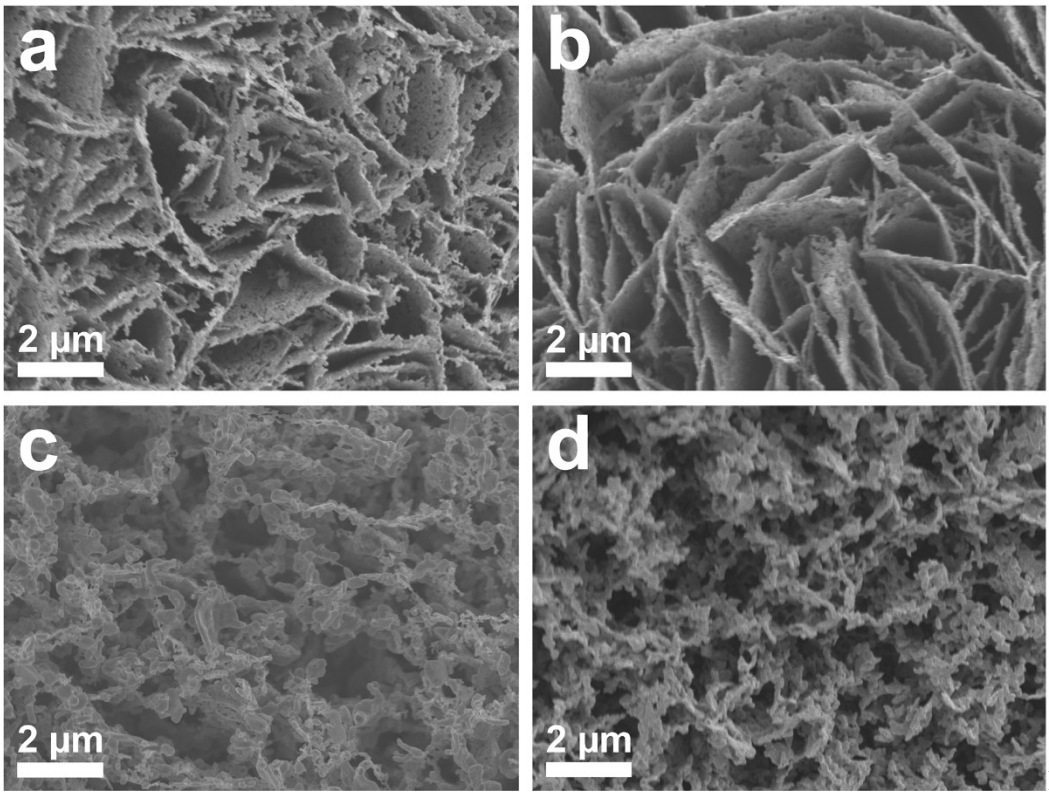

Figure S18. SEM images of the Ni_3N/NF prepared under different nitridation treating conditions (a) 340 °C for 2h; (b) 380 °C for 1h; (c) 380 °C for 3h and (d) 420 °C for 2h.

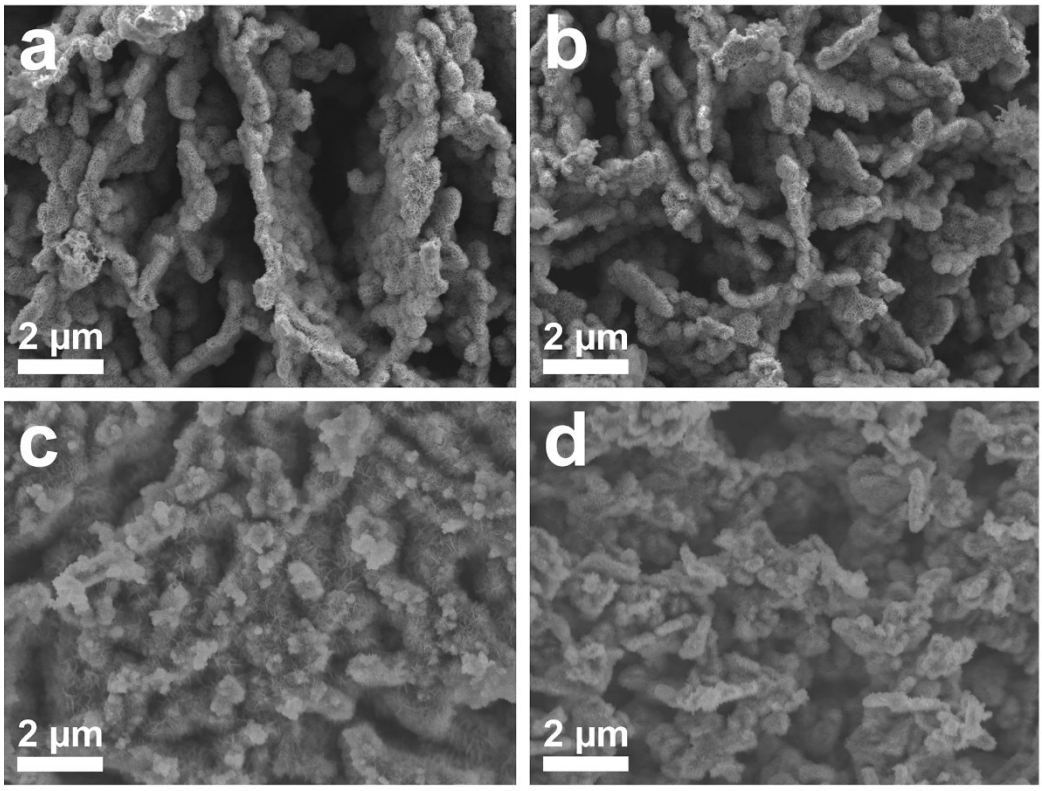

Figure S19. SEM images of the NiFe LDH@Ni_3N/NF synthesized with different Ni_3N/NF (a) 340 °C for 2h; (b) 380 °C for 1h; (c) 380 °C for 3h and (d) 420 °C for 2h.

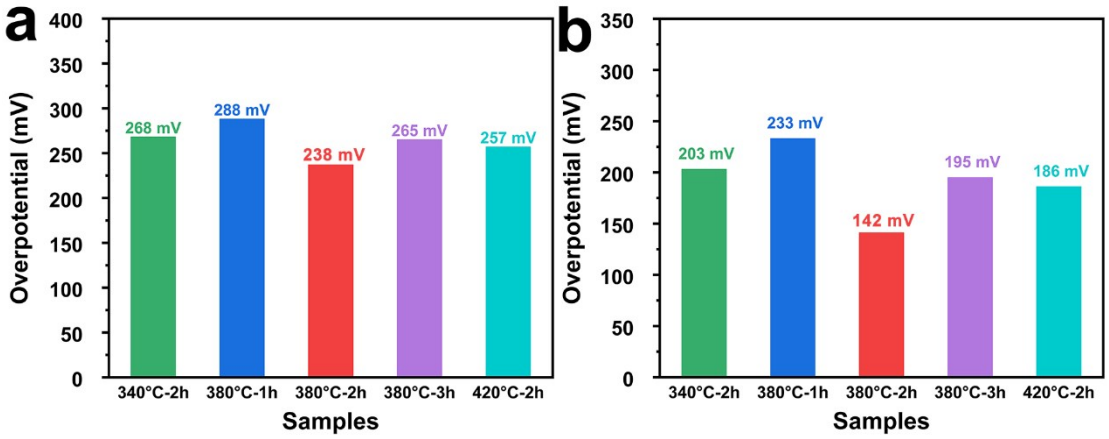

Figure S20. Comparison of overpotentials at a current density of 100 mA cm^{-2} for (a) OER and (b) HER of the NiFe LDH@Ni_3N/NF catalysts synthesized with different Ni_3N/NF.

To optimize the preparation conditions of Ni_3N/NF, we have further changed the nitridation temperature and time (e.g., 340 °C for 2h, 380 °C for 1h, 380 °C for 3h, and 420 °C for 2h).

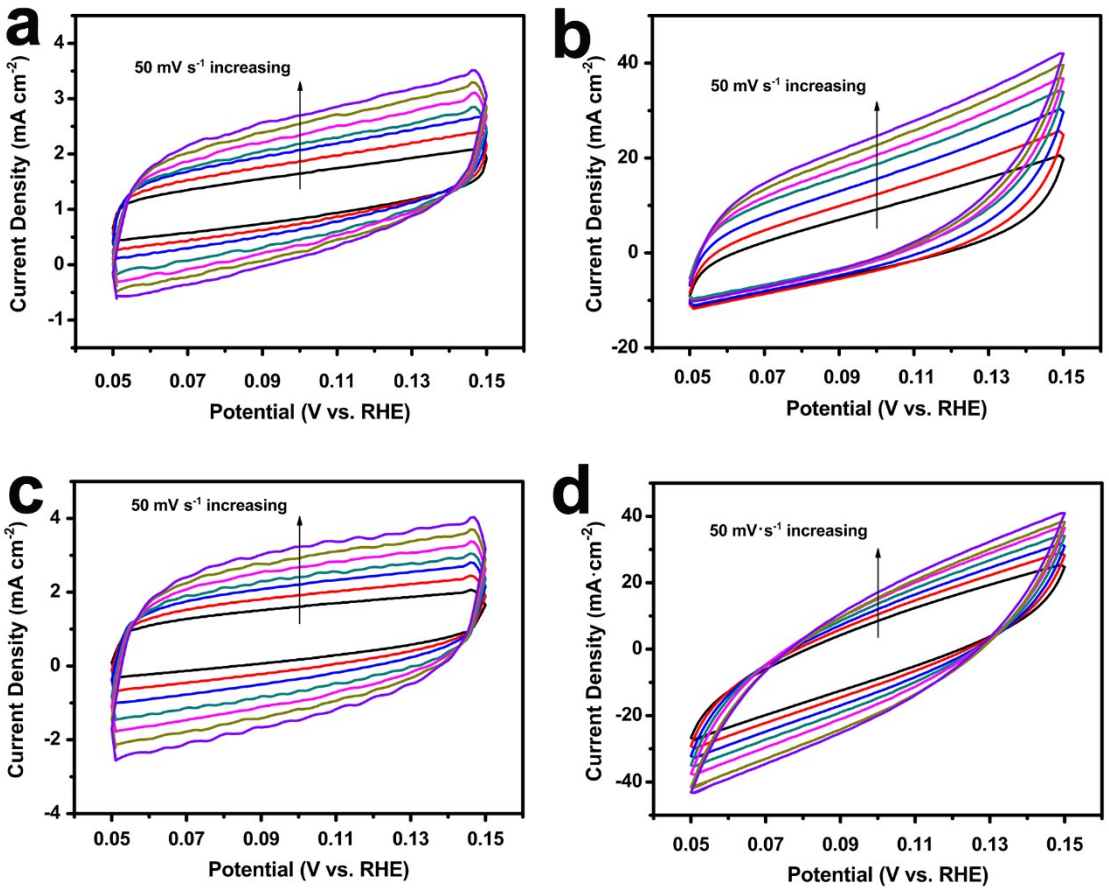

Figure S21. CV curves of the (a) blank NF; (b) Ni_3N/NF; (c) NiFe LDH/NF and (d) NiFe LDH@Ni_3N/NF measured at different scan rates.

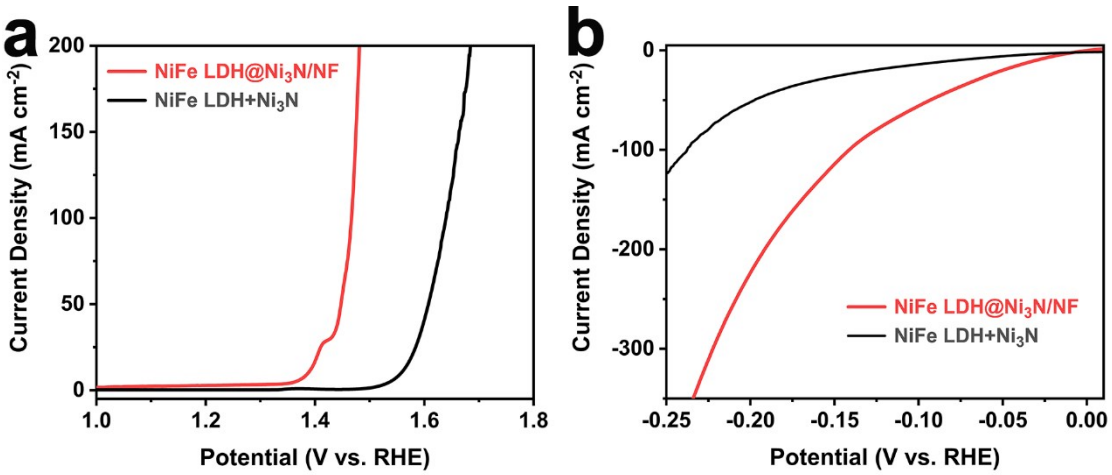

Figure S22. (a) OER and (b) HER polarization curves of the NiFe LDH@Ni_3N/NF electrode compared to the physical mixture of NiFe LDH and Ni_3N casted on the Ni foam.

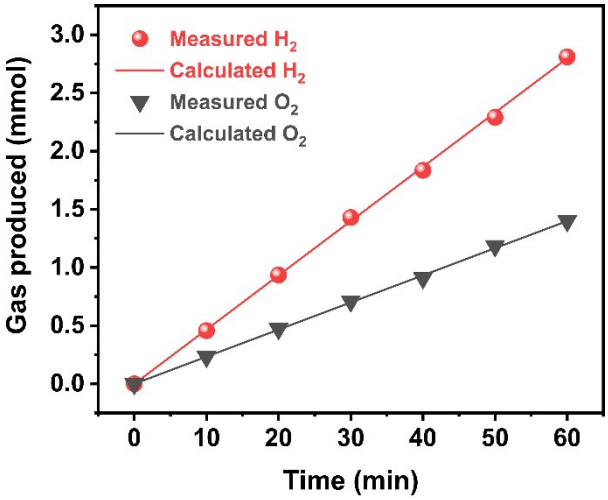

Figure S23. Experimental and theoretical amounts of H_2 and O_2 production by the NiFe LDH@Ni_3N/NF//NiFe LDH@Ni_3N/NF electrolyzer for overall water splitting at 500 mA cm^{-2}.

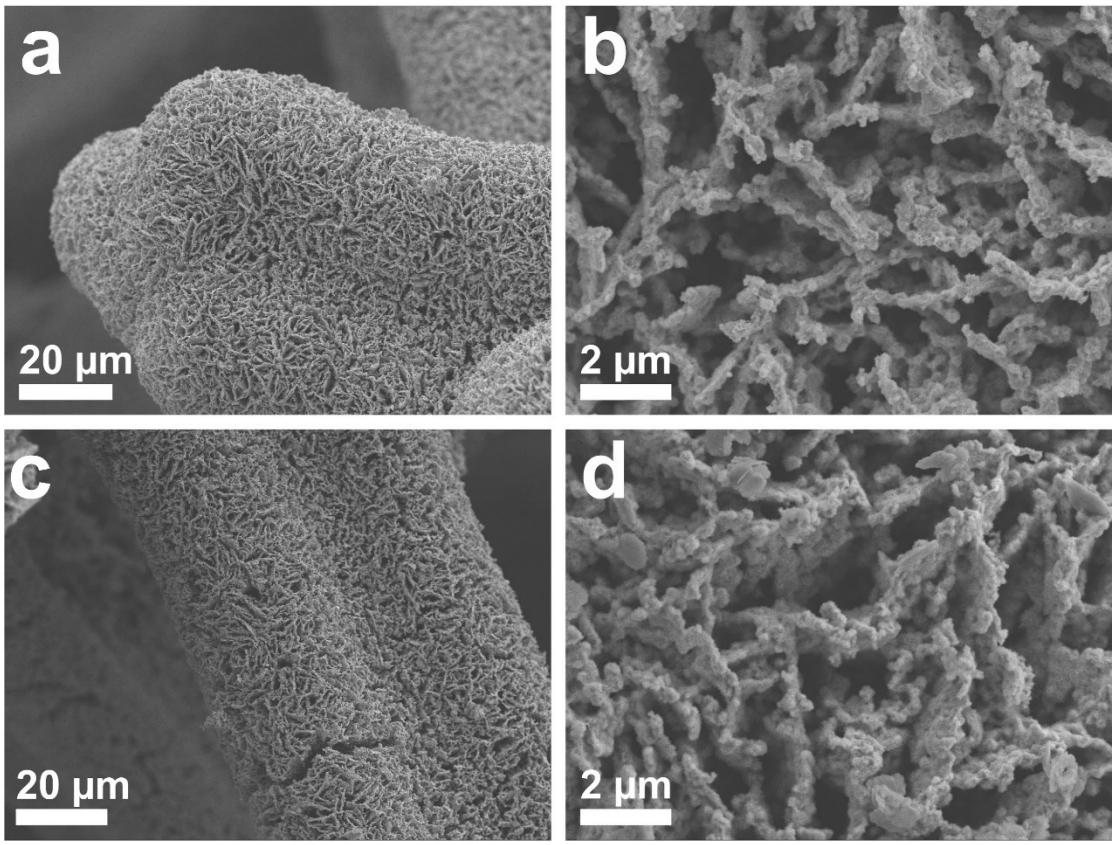

Figure S24. SEM images of the NiFe LDH@Ni_3N/NF after (a-b) OER and (c-d) HER stability tests.

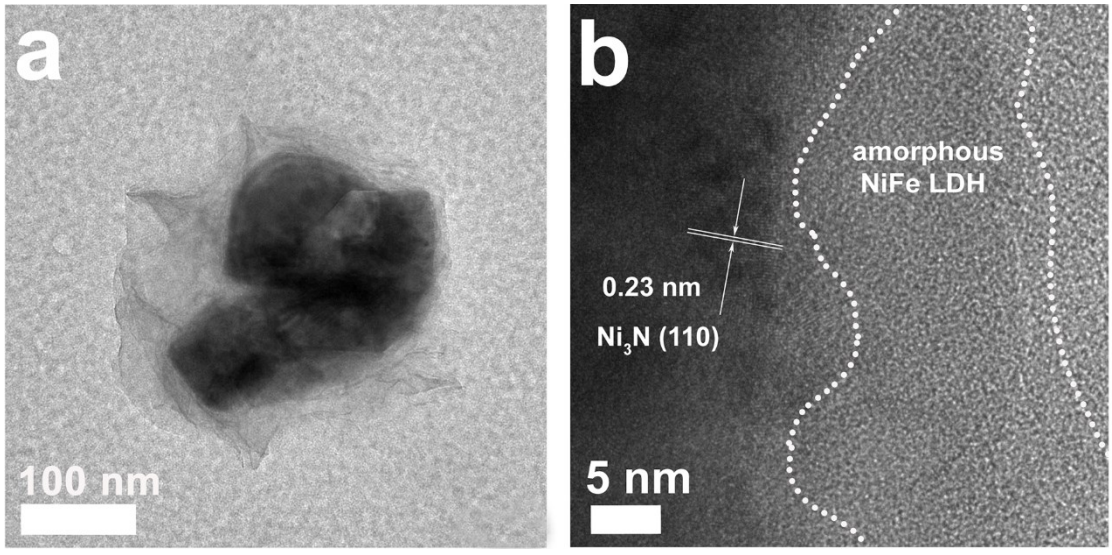

Figure S25. (a) TEM and (b) HRTEM images of the NiFe LDH@Ni_3N/NF after OER stability test.

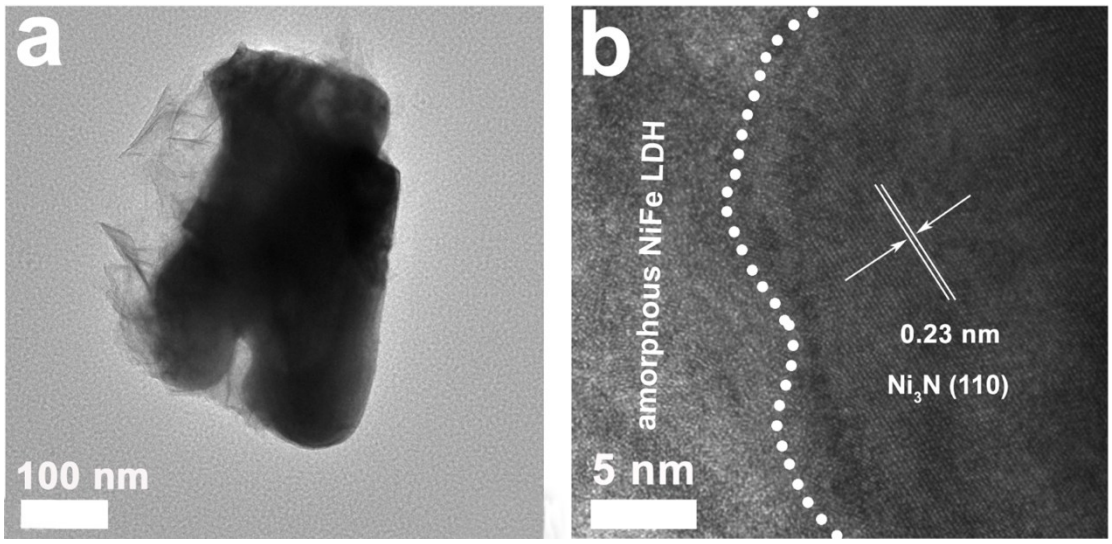

Figure S26. (a) TEM and (b) HRTEM images of the NiFe LDH@Ni_3N/NF after HER stability test.

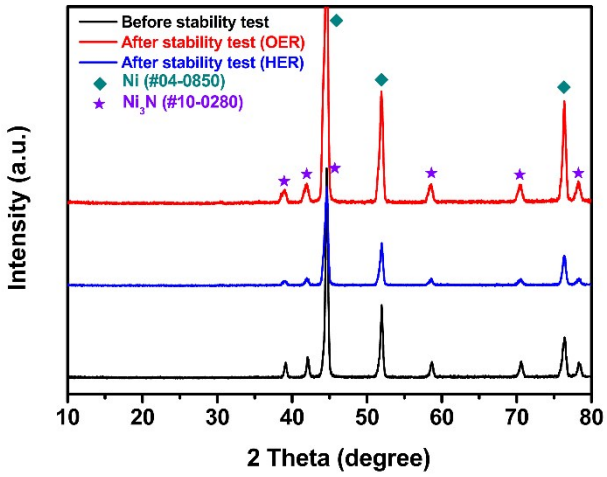

Figure S27. XRD patterns of the NiFe LDH@Ni_3N/NF before and after stability tests.

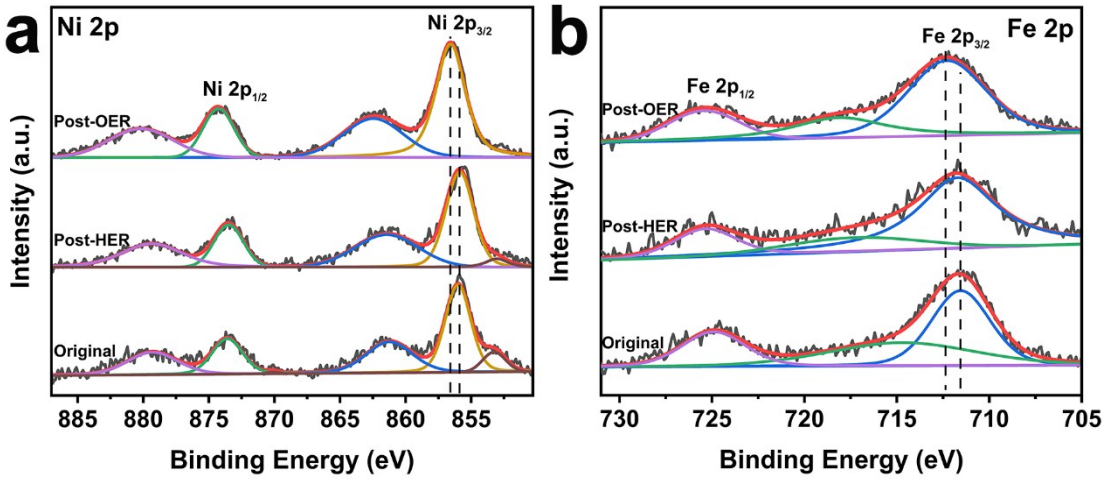

Figure S28. High-resolution XPS spectra of (a) Ni 2p and (b) Fe 2p for the NiFe LDH@Ni_3N/NF before and after stability tests.

Table S1. The mass loadings of different NiFe LDH@Ni_3N with different electrodeposition times on the Ni foam and the exact mass ratio of NiFe LDH to Ni_3N.

Mass loadings / Samples	Ni_3N (mg cm^{-2})	NiFe LDH (mg cm^{-2})	total (mg cm^{-2})	mass ratio (Ni_3N/NiFe LDH)
Ni_3N/NF	3.21	-	3.21	-
30-NiFe LDH@Ni_3N/NF	3.21	0.31	3.52	10.35:1
60-NiFe LDH@Ni_3N/NF	3.21	0.37	3.58	8.68:1
NiFe LDH@Ni_3N/NF	3.21	0.82	4.03	3.91:1
180-NiFe LDH@Ni_3N/NF	3.21	1.59	4.80	2.02:1
600-NiFe LDH@Ni_3N/NF	3.21	4.05	7.26	0.79:1

Table S2. OER performances of Ni and Fe based electrocatalysts in 1 M KOH electrolyte: this work vs. literatures.

References	Catalyst	j (mA cm^{-2})	η (mV)	Stability Test	Faradaic efficiency
This work	NiFe LDH@Ni_3N/NF	100 500	238 275	100 h at 500 mA cm^{-2}	100%
14	NFN-MOF/NF	10 250 500	240 335 360	30 h at 250 and 500 mA cm^{-2}	100%
30	NiFe-LDH/MXene/NF	500	300	70 h at 100 mA cm^{-2}	98%
55	CoNi/$CoFe_2O_4$/NF	10 100 500	230 290 330	48 h at 10 and 100 mA cm^{-2}	99%
56	Sn-Ni_3S_2/NF	100 500	267 440	60 h at 100 and 500 mA cm^{-2}	100%
57	Fe-CoP/NF	500	295	30 h at 500 mA cm^{-2}	100%
58	Ni@NiFe LDH	100 300 500	269 315 349	24 h at 10 mA cm^{-2}	100%
59	P-Co-Ni-S/NF	100 500	292 449*	16 h at 10 mA cm^{-2}	NA
60	NF-Ni_3S_2/MnO_2	10 100 500	260 348 431*	40 h at 100 mA cm^{-2}	NA
61	NiFe/$NiCo_2O_4$/NF	10 500	240* 321*	11 h at 10 and 50 mA cm^{-2}	99.8%
62	NixCo_3-xS_4/Ni_3S_2/NF	100 500	320 475	30 h at 10 mA cm^{-2}	100%
63	MFN-MOFs/NF	50 500	235 294	NA	100%
64	$Ni_{0.3}Co_{0.7}$-9AC-AD/NF	100	350	30 h at 70 mA cm^{-2}*	NA
65	$FeSe_2$-180 °C	10	330	70 h at 37 mA cm^{-2}*	100%

* The value is calculated from the curves shown in the literatures.

Table S3. TOF for different samples at overpotential of 300 mV corresponding to OER.

Catalyst	TOF（s^{-1}）
Ni_3N/NF	0.010
NiFe LDH/NF	0.189
30-NiFe LDH@Ni_3N/NF	0.204
60-NiFe LDH@Ni_3N/NF	0.560
NiFe LDH@Ni3N/NF	0.579
180-NiFe LDH@Ni_3N/NF	0.502
600-NiFe LDH@Ni_3N/NF	0.395

Table S4. HER performances of Ni foam-based electrocatalysts in 1 M KOH electrolyte: this work vs. literatures.

References	Catalyst	j (mA cm^{-2})	η (mV)	Stability Test	Faradaic efficiency
This work	NiFe LDH@Ni_3N/NF	100 500	142 265	100 h at 500 mA cm^{-2}	100%
14	NFN-MOF/NF	10 250 500	87 256 293	30 h at 250 and 500 mA cm^{-2}	100%
30	NiFe-LDH/MXene/NF	500	205	280 h at 10 mA cm^{-2}	98%
55	CoNi/$CoFe_2O_4$/NF	10 100	82 189	48 h at 10 and 100 mA cm^{-2}	99%
56	Sn-Ni_3S_2/NF	100 300	171 279	60 h at 200 mA cm^{-2}	99.7%
57	Fe-CoP/NF	10	78	30 h at 10 mA cm^{-2}	100%
58	Ni@NiFe LDH	100	233	24 h at 10 mA cm^{-2}	100%
59	P-Co-Ni-S/NF	100 500	187 287*	16 h at 10 mA cm^{-2}	NA
60	NF-Ni_3S_2/MnO_2	10 100	102 197	48 h at 40 mA cm^{-2}	NA
61	NiFe/$NiCo_2O_4$/NF	10 100	105 204*	10 h at 20 mA cm^{-2}	NA
62	$NixCo_3$-xS_4/Ni_3S_2/NF	100 500	258 432	50 h at 10 mA cm^{-2}	100%
63	MFN-MOFs/NF	10 500	79 234	NA	100%
64	$Ni_{0.3}Co_{0.7}$-9AC-AD/NF	10 100	143 232	30 h at 4 mA cm^{-2}*	NA

* The value is calculated from the curves shown in the literatures.

Table S5. TOF for different samples at overpotential of 100 mV corresponding to HER.

Catalyst	TOF（s^{-1}）
Ni_3N/NF	0.050
NiFe LDH/NF	0.031
30-NiFe LDH@Ni_3N/NF	0.058
60-NiFe LDH@Ni_3N/NF	0.104
NiFe LDH@Ni_3N/NF	0.157
180-NiFe LDH@Ni_3N/NF	0.070
600-NiFe LDH@Ni_3N/NF	0.062

Table S6. Overall water splitting performances of Ni foam-based bifunctional electrocatalysts in 1 M KOH electrolyte: this work vs. literatures.

References	Catalyst	j (mA cm^{-2})	Potential (V)	Stability Test
This work	NiFe LDH@Ni_3N/NF	100 500	1.63 1.80	100 h at 500 mA cm^{-2}
14	NFN-MOF/NF	10 250 500	1.56 1.84 1.96	30 h at 250 and 500 mA cm^{-2}
30	NiFe-LDH/MXene/NF	10 500	1.51 1.75	200 h at 100 mA cm^{-2}
55	CoNi/$CoFe_2O_4$/NF	10 100	1.57 1.75	48 h at 10 and 100 mA cm^{-2}
56	Sn-Ni_3S_2/NF	10 100 500	1.46 1.77* 2.26	45 h at 10 mA cm^{-2}
57	Fe-CoP/NF	10 100	1.49 1.61*	50 h at 10 mA cm^{-2}
58	Ni@NiFe LDH	10 100	1.53 1.78	24 h at 10 mA cm^{-2}
59	P-Co-Ni-S/NF	10	1.60	20 h at 10 mA cm^{-2}
60	NF-Ni_3S_2/MnO_2	10 100	1.52 1.61*	48 h at 100 mA cm^{-2}
61	NiFe/$NiCo_2O_4$/NF	10 100	1.67 1.88*	10 h at 20 mA cm^{-2}
62	Ni_xCo_3-xS_4/Ni_3S_2/NF	10 100	1.53 1.80	200 h at 10 and 100 mA cm^{-2}
63	MFN-MOFs/NF	10 500	1.50 1.80	100 h at 100 and 500 mA cm^{-2}
64	$Ni_{0.3}Co_{0.7}$-9AC-AD/NF	10 100	1.56 1.72*	30 h at 11 mA cm^{-2}*

* The value is calculated from the curves shown in the literatures.